

# Unusual Molecular Conformations in Fluorinated, Contorted Hexabenzocoronenes

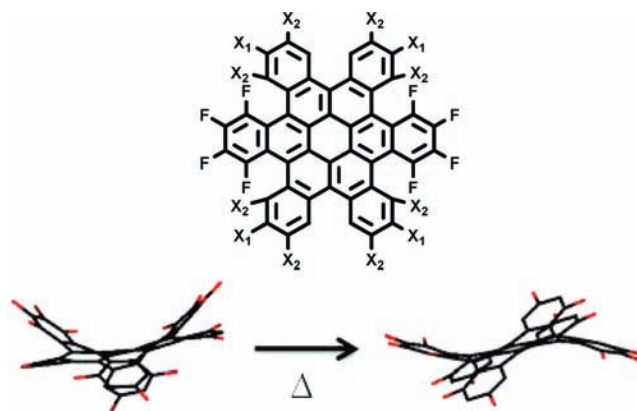
Yueh-Lin Loo,<sup>\*,†</sup> Anna M. Hiszpanski,<sup>†</sup> Bumjung Kim,<sup>‡</sup> Sujun Wei,<sup>‡</sup> Chien-Yang Chiu,<sup>‡</sup> Michael L. Steigerwald,<sup>‡</sup> and Colin Nuckolls<sup>\*,‡</sup>

Department of Chemical & Biological Engineering, Princeton University, Princeton, New Jersey 08544, United States, and Department of Chemistry and the Center for Electronics of Molecular Nanostructures, Columbia University, New York, New York 10027, United States

lloo@princeton.edu; cn37@columbia.edu

Received August 25, 2010

## ABSTRACT



Fluorinated, contorted hexabenzocoronenes (HBCs) have been synthesized in a facile manner via Suzuki–Miyaura coupling of fluorinated phenyl boronic acids followed by photocyclization and Scholl cyclization. In addition to the molecular conformation observed in previous HBC derivatives, close-contact fluorine–fluorine intramolecular interactions result in a metastable conformation not previously observed. Heating the metastable HBCs above 100 °C irreversibly converts them to the stable conformation, suggesting that the metastable conformation arises from a kinetically arrested state during cyclization.

Hexabenzocoronenes (HBCs) have attracted significant scientific attention given their interesting electronic and self-assembly properties. Both planar and contorted HBCs, for example, have been incorporated as active layers in organic thin-film transistors; devices comprising unsubstituted planar HBC<sup>1</sup> and dodecyloxy-substituted contorted HBC<sup>2</sup> exhibit hole mobilities of the order of 10<sup>0</sup> and 10<sup>-2</sup> cm<sup>2</sup>/V·s,

respectively. These materials also have a strong tendency to self-assemble into supramolecular structures; both planar and contorted HBCs readily pack in a columnar fashion to generate nanorods and wires affording field-effect transistors.<sup>1–3</sup> Unlike planar HBCs, whose structures resemble small sections of graphene, the molecular conformation of contorted HBCs is distorted from planarity by 20° on its

<sup>†</sup> Princeton University.

<sup>‡</sup> Columbia University.

(1) van de Cratts, A. M.; Warman, J. M.; Fechtenkötter, A.; Brand, J. D.; Harbison, M. A.; Müllen, K. *Adv. Mater.* **1999**, *11*, 1469–1472.

(2) Xiao, S.; Myers, M.; Miao, Q.; Sanaur, S.; Pang, K.; Steigerwald, M. L.; Nuckolls, C. *Angew. Chem., Int. Ed.* **2005**, *117*, 7556–7560.

(3) Xiao, S.; Tang, J.; Beetz, T.; Guo, X.; Tremblay, N.; Siegrist, T.; Zhu, Y.; Steigerwald, M. L.; Nuckolls, C. *J. Am. Chem. Soc.* **2006**, *128*, 10700–10701.

periphery due to steric congestion between the proximal C–H bonds. This doubly concave conformation can thus provide unique opportunities for complexation with geometrically complementary compounds, such as C<sub>60</sub>.<sup>4</sup>

The addition of fluorenyl units<sup>5</sup> and oligothiophenes<sup>6</sup> at the peripheral aromatic rings of planar and contorted HBCs, respectively, has been shown to alter the optical absorbance and the HOMO and LUMO energy levels of the parent compound in addition to improving the molecular packing in the solid state. In the same vein, select fluorination of the outer aromatic rings of planar HBC is found to enhance the molecule's electron-withdrawing nature;<sup>7</sup> fluorinated planar HBC is reported to transport electrons with a mobility of 10<sup>-2</sup> cm<sup>2</sup>/V·s.<sup>8</sup> More interestingly, this compound is shown to adopt a face-to-face type packing motif in the solid state rather than the herringbone structure that is found in its parent compound due to the larger van der Waals radius of fluorine.<sup>8</sup> Inspired by the work of Mori et al.,<sup>8</sup> we wanted to examine the influence of fluorine–fluorine intramolecular interactions on the molecular conformation of contorted HBCs given their already-unusual doubly concave conformation.

In this study, we report the synthesis and characterization of a series of contorted HBCs with differing amounts of fluorination on its exterior aromatic rings.<sup>9</sup> Functionalized contorted HBCs have been previously realized via double Barton–Kellogg reactions of the appropriate pentacenequinones followed by photocyclization or Scholl cyclization.<sup>10</sup> The synthetic scheme used here is different than those employed in the past and is shown in Scheme 1. We carried

out a double Corey–Fuchs<sup>11</sup> reaction on fluorinated pentacenequinone to provide a precursor to the fluorinated, contorted HBCs shown in Figure 1. This reaction yields a

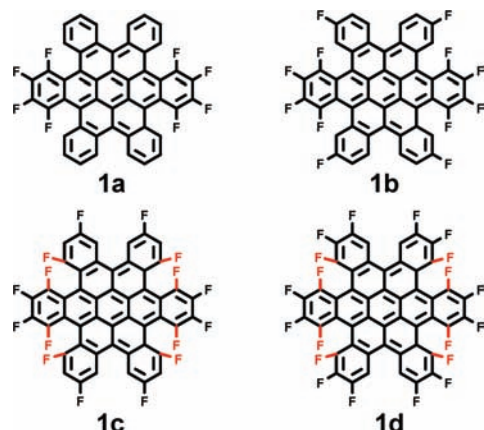


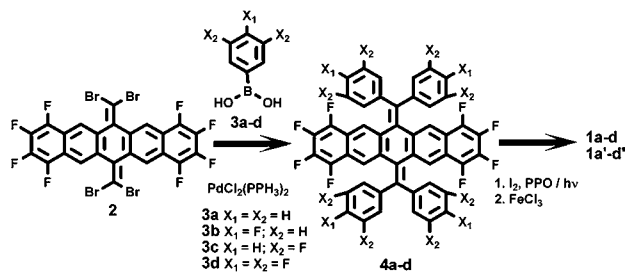
**Figure 1.** Chemical structures of 8F- (**1a**), 12F- (**1b**), 16F- (**1c**), and 20F-HBC (**1d**). Close fluorine–fluorine intramolecular contacts (<2.6 Å) are highlighted in red for **1c** and **1d**.

tetrabrominated intermediate, **2**. Subjecting **2** to a Suzuki–Miyaura<sup>12</sup> reaction with the appropriate fluorinated phenyl boronic acid (**3a–d**) yielded the desired bisolefin compound, **4a–d**. We then employed the Katz-modified Mallory photocyclization<sup>13,14</sup> on **4a–d**; the products from these reactions consisted of a mixture of half-cyclized and fully cyclized HBCs (**1a–d**). Given the solubility differences between the half- and fully cyclized HBCs, we isolated the half-cyclized products and imposed upon them Scholl cyclizations per Plunkett et al.<sup>9</sup> to yield the fully cyclized products, **1a'–d'**. Given the wide availability of functionalized phenyl boronic acids, this route brings about tremendous flexibility and modularity to the synthesis of contorted HBCs with different substitution.

X-ray crystallography indicates that the fluorinated, contorted HBCs that result from photocyclization adopt molecular conformations that are not significantly different from that of their hydrogen-substituted counterpart. They adopt, for example, the doubly concave conformation that characterizes contorted hexabenzocoronenes.<sup>2–4</sup> At first blush, it thus appears that substituting hydrogens with fluorines on the peripheral aromatic rings of contorted HBCs does not affect their molecular conformations.

The <sup>1</sup>H NMR spectrum of 8F-HBC obtained upon Scholl cyclization (**1a'**) is in all respects identical to that of 8F-HBC obtained after photocyclization (**1a**), indicating that **1a'** and **1a** are chemically and conformationally indistinguishable. We

**Scheme 1.** General Strategy for Synthesizing Fluorinated, Contorted HBCs



(4) Tremblay, N. J.; Gorodetsky, A. A.; Cox, M. P.; Schiros, T.; Kim, B.; Steiner, R.; Bullard, Z.; Sattler, A.; So, W.-Y.; Itoh, Y.; Toney, M. F.; Ogasawa, H.; Ramirez, A. P.; Kymissis, I.; Steigerwald, M. L.; Nuckolls, C. *ChemPhysChem* **2010**, *11*, 799–803.

(5) Wong, W. W. H.; Singh, T. B.; Vak, D.; Pisula, W.; Yan, C.; Feng, X.; Williams, E. L.; Chan, K. L.; Mao, Q.; Jones, D. J.; Ma, C.-Q.; Müllen, K.; Bäuerle, P.; Holmes, A. B. *Adv. Funct. Mater.* **2010**, *20*, 927–938.

(6) Unpublished data.

(7) Etani, S.; Kaji, T.; Ikeda, S.; Mori, T.; Kikuzawa, Y.; Takeuchi, H.; Saiki, K. *J. Phys. Chem. C* **2009**, *113*, 6202–6207.

(8) Mori, T.; Kikuzawa, Y.; Takeuchi, H. *Org. Electron.* **2008**, *9*, 328–332.

(9) Gorodetsky, A. A.; Chiu, C. Y.; Schiros, T.; Palma, M.; Sattler, W.; Kymissis, I.; Steigerwald, M.; Nuckolls, C. *Angew. Chem., Int. Ed.* published online Sept. 16, 2010; DOI: 10.1002/anie.201004055.

(10) Plunkett, K. N.; Godula, K.; Nuckolls, C.; Tremblay, N.; Whalley, A. C.; Xiao, S. *Org. Lett.* **2009**, *11*, 2225–2228.

(11) Neidlein, R.; Winter, M. *Synthesis* **1998**, *9*, 1362–1366.

(12) (a) Miyaura, N.; Suzuki, A. *Chem. Rev.* **1995**, *95*, 2457–2483. (b) Bauer, A.; Miller, M. W.; Vice, S. F.; McCombie, S. W. *Synlett* **2001**, *2*, 254–256.

(13) Mallory, F. B.; Wood, C. S.; Gordon, J. T.; Lindquist, L. C.; Savitz, M. L. *J. Am. Chem. Soc.* **1962**, *84*, 4361–4362.

(14) Liu, L. B.; Yang, B. W.; Katz, T. J.; Poindexter, M. K. *J. Org. Chem.* **1991**, *56*, 3769–3775.

found this observation to hold true for 12F-HBC also. This observation, however, does not hold true for 16F-HBC or 20F-HBC, both of which have close intramolecular fluorine–fluorine contacts (<2.6 Å). The NMR spectra of 16F-HBC obtained after photocyclization (**1c**) and after Scholl cyclization (**1c'**) are shown in Figure 2. We observe two sets of resonances

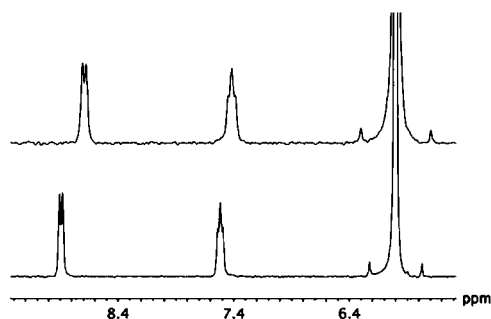


**Figure 2.**  $^1\text{H}$  NMR spectra of **1c** (top) and **1c'** (bottom). The spectra have been corrected against the reference peak of tetrachloroethane at 6.00 ppm.

associated with the two proton environments in 16F-HBC. The triplet at 7.4 ppm in the NMR spectrum of **1c** is assigned to the protons on the peripheral aromatic rings that are sandwiched between fluorine substituents on the same rings. The doublet at 8.7 ppm is attributed to the less shielded protons of 16F-HBC. Integrating the proton resonances confirms equal contributions to the NMR spectrum of 16F-HBC. The NMR spectrum of **1c'** appears to be similar to that of **1c**, but both the triplet and the doublet in the spectrum of **1c'** are shifted downfield relative to those of **1c** at the same concentration. Comparison of the placement of the proton resonance of the reference solvent (tetrachloroethane;  $\delta = 6.0$  ppm) indicates that this downfield shift seen in the spectrum of **1c'** is not an experimental artifact; rather, it reflects real differences in the molecular conformations of **1c** and **1c'**. We have also carried out NMR experiments on mixtures of **1c** and **1c'**; both sets of resonances are present, further confirming that the differences in chemical shifts stem from differences in molecular conformations.

Figure 3 shows the molecular conformations of **1c** and **1c'** observed in the crystal structure of each. We observe



**Figure 3.** Side view of **1c** (left) and **1c'** (right) based on X-ray crystallography. Fluorine is depicted in red. Hydrogens have been removed for clarity. The stick figures below illustrate the conformations of the ring planes originating from the fluorinated pentacene-quinone precursor.

that the outer aromatic rings in **1c** alternate into and out of the plane defined by the coronene core, resulting in a doubly concave structure that is similar to those exhibited by other contorted HBCs.<sup>2–4</sup> The molecular conformation of **1c'**, on the other hand, has not previously been observed. In particular, the perfluorinated outer aromatic rings originating from fluorinated pentacenequinone are contorted out of the plane defined by the coronene core in the same direction, resulting in a saddle-like conformation (see the molecular models in Figure 3 for comparison of the positions of the outer aromatic rings originating from the fluorinated pentacenequinone precursor). The exterior aromatic rings introduced by coupling with **3c** are displaced in the opposite direction, presumably to minimize close fluorine–fluorine intramolecular contact (highlighted in red for 16F-HBC in Figure 1). In the solid state, both **1c** and **1c'** adopt monoclinic crystal structures having the  $P2_1/C$  space group with slightly different unit cell dimensions.<sup>15</sup>

Minimization of free energy of these molecular conformations via density functional theory (DFT) calculations indicates that the armchair structure of **1c** depicted in the left of Figure 3 sits at a lower energy compared to the saddle structure of **1c'** (right of Figure 3). Indeed, variable-temperature NMR experiments carried out on **1c'** indicate that heating above 100 °C induces a transformation in molecular conformation to that adopted by **1c**. This transformation is irreversible; cooling to room temperature does not allow reversion back to its original conformation.

To quantitatively examine the transformation from the metastable conformation of **1c'** to that of **1c**, we monitored the kinetics of this process isothermally via NMR. Figure 4

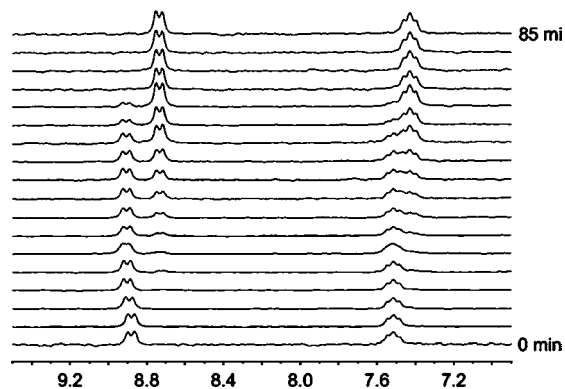


**Figure 4.**  $^1\text{H}$  NMR spectra acquired in 5 min intervals during isothermal transformation of **1c'** at 110 °C.

contains sequential NMR spectra collected of **1c'** at 110 °C in 5 min intervals. As time progresses, we observe a steady increase in the intensities of the proton resonances associated with **1c**; this increase occurs concomitantly with a decrease in intensity of the original proton resonances associated with

(15) The unit cell dimensions for **1c**:  $a = 12.966$  Å;  $b = 8.566$  Å;  $c = 14.310$  Å;  $\beta = 90.27^\circ$ . The unit cell dimensions for **1c'**:  $a = 14.740$  Å;  $b = 13.624$  Å;  $c = 16.060$  Å;  $\beta = 99.12^\circ$ .

**1c'**. In fact, collapsing the spectra in Figure 4 reveals an isosbestic point at 7.47 ppm indicating that one species is converting into another. The conversion from the metastable to stable conformations is complete after 85 min. We also tracked the growth of the proton resonances associated with the more stable conformation; this quantity is plotted in Figure 5 for the isothermal transformation at 110 °C. The

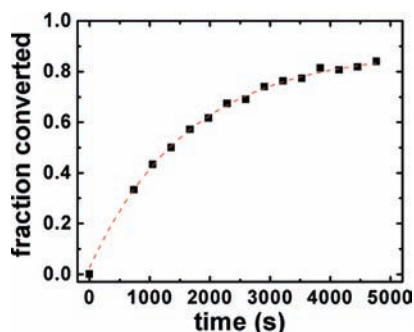


**Figure 5.** Rate of transformation from the metastable to the stable conformations of 16F-HBC at 110 °C. The red line represents the first-order fit to the data.

data are well described by first-order kinetics; fitting yields a rate constant of  $0.0004\text{ s}^{-1}$  or a characteristic half time of 1700 s. Fitting the rate constants obtained at several temperatures to the Arrhenius equation yielded an energy barrier of 39 kcal/mol for this transformation. Given that the *gauche-to-trans* transformation of C–C bonds is estimated to require 3–6 kcal/mol,<sup>16</sup> an energy barrier of 39 kcal/mol seems reasonable for the transformation between the two conformations of 16F-HBC given the significant rearrangement of C–C bonds that needs to take place.

We note that the fully cyclized 20F-HBC product upon photocyclization (**1d**) adopts a molecular conformation that resembles that of **1c** and those of prior contorted HBCs. The Scholl cyclized product of **1d'**, akin to **1c'**, adopts a molecular conformation that is less stable than that of **1d** and undergoes transformation back to the more stable form on heating. Examining the chemical structures of 16F- and 20F-HBC, we notice that both compounds share close fluorine–fluorine intramolecular contacts (highlighted red in Figure 1). We believe it is the steric hindrance between adjacent fluorinated aromatic rings during ring closure that gives rise to the different molecular conformations.<sup>17</sup> During photocycliza-

tion, the bisolefin intermediates **4a–d** first undergo half-cyclization before complete ring closure.<sup>9</sup> Given the numerous degrees of rotational freedom of the Suzuki–Miyaura intermediates, the half-cyclized species are likely to sample a number of conformations. We speculate that only conformations having minimal steric hindrance between fluorines on adjacent aromatic rings are capable of complete ring closure during photocyclization. Ring closure of the remaining half-cyclized species—due to additional fluorine–fluorine steric hindrance—only occurs during the more energetic Scholl cyclization. This hypothesis is consistent with our observation that photocyclization always yields a mixture of half- and fully cyclized fluorinated, contorted HBCs. Extending the photocyclization reaction does not further convert the half-cyclized product into the final product.

In summary, we have demonstrated a facile and modular method for synthesizing contorted HBC having varying extents of fluorination. Close fluorine–fluorine intramolecular contact results in a metastable molecular conformation not previously observed. Our study highlights the intricacies of fluorine substitution and hints at the possibility of accessing unusual and metastable molecular conformations through fine-tuning of intramolecular steric hindrance.

**Acknowledgment.** We thank Rawad Hallani and Prof. John Anthony (Chemistry, University of Kentucky) for the fluorinated pentacenequinone and Wesley Sattler (Chemistry, Columbia) for X-ray crystallography. Y.L.L. acknowledges financial support from the PIRE Program (DMR-0730243) and the MRSEC Program through Princeton’s PCCM (DMR-0819860) at the NSF and the Photovoltaics Program at the ONR (N000140811175). A.M.H. is supported by an NSF Nanotechnology for Clean Energy IGERT Traineeship (0903661). Funding through CHE-0619638 for the acquisition of the X-ray diffractometer is appreciated. Portions of this work (CN) were funded by the Center for Re-Defining Photovoltaic Efficiency Through Molecule Scale Control, an Energy Frontier Research Center funded by the U.S. DOE, Office of Science, Office of Basic Energy Sciences (DESC0001085), and by the Chemical Sciences, Geosciences and Biosciences Division (DEFG02-01ER15264).

**Supporting Information Available:** Procedures and NMR spectra of compounds. CIF files for **1c** and **1c'**. This material is available free of charge via the Internet at <http://pubs.acs.org>.

OL102016M

(16) Wiberg, K. B.; Murcko, M. A. *J. Am. Chem. Soc.* **1988**, *110*, 8029–8038.

(17) Coates, G. W.; Dunn, A. R.; Henling, L. M.; Dougherty, D. A.; Grubbs, R. H. *Angew. Chem., Int. Ed.* **1997**, *36*, 248–251.